Microrheology of viscoelastic fluids containing light-scattering inclusions

Catalina Haro-Pérez,[1] Efrén Andablo-Reyes,[1] Pedro Díaz-Leyva,[1] and José Luis Arauz-Lara[1,2]
[1]*Instituto de Física "Manuel Sandoval Vallarta," Universidad Autónoma de San Luis Potosí, Álvaro Obregón 64, 78000 San Luis Potosí, S.L.P., Mexico*
[2]*Departamento de Física, CINVESTAV, Avenida IPN 2508, Colonia Zacatenco, 07360 México, D. F., Mexico*
(Received 10 November 2006; published 30 April 2007)

The microrheology of viscoelastic fluids containing light-scattering inclusions is measured by depolarized dynamic light scattering (DDLS) from optically anisotropic spherical colloidal probes. The anisotropy of the probes allows us to measure both their translational and the rotational mean squared displacements simultaneously, and DDLS allows us to suppress the light scattered from the inclusions. The storage and loss moduli are determined from both mean squared displacements and the results compared with mechanical measurements.

DOI: 10.1103/PhysRevE.75.041505 PACS number(s): 83.10.Mj, 83.60.Bc, 78.35.+c

I. INTRODUCTION

Soft materials abound in nature and in industrial products, from biological materials (for instance, proteins or DNA solutions) to polymeric solutions, gels, paints, cosmetics, foods, etc. Thus the development of methods to characterize their mechanical properties (among others) is of wide interest. Microrheological methods are currently used to characterize the mechanical properties of such systems at frequencies and space scales unattainable to mechanical instruments, and to characterize the mechanical properties of very small systems, such as the cytoplasm of living cells [1–4]. Microrheology is based on a frequency analysis of the diffusive motion of probe colloidal particles embedded in the material of interest [5]. It uses as a theoretical framework a generalization of the Stokes-Einstein relation between the translational motion of the probe particles and the local mechanical properties of the host medium, i.e.,

$$G^*(\omega) = \frac{k_B T}{i\omega\pi a\langle \Delta \boldsymbol{r}^2(\omega)\rangle}, \tag{1}$$

where $\langle \Delta \boldsymbol{r}^2(w)\rangle$ is the frequency dependent mean squared displacement obtained from that in real time $\langle \Delta \boldsymbol{r}^2(t)\rangle$, ω is the frequency of shearing, $k_B T$ is the thermal energy, and a is the particle's radius. $G^*(\omega)$ represents the complex shear modulus, whose real part $G'(\omega)$ is the elastic or storage modulus and the imaginary part $G''(\omega)$ is the viscous or loss modulus [6]. Most of the current microrheological methods are based on the measurement and analysis of the translational motion of probe particles in the host medium [6–8]. Nevertheless, the rotational motion also probes the mechanical response of the medium, in this case to torsional shear strains, and it can be used as an alternative and/or complementary way to determine the rheology of soft materials [9]. For spherical probes, one can also use a simple generalization of the Stokes-Einstein relation between the mechanical properties of the host and the rotational diffusion, which for small angular displacements is characterized by the mean squared angular displacement $\langle \Delta\theta^2(t)\rangle$, where $\Delta\theta(t)$ is the angular displacement of the particle's director with two degrees of freedom, i.e.,

$$G^*(\omega) = \frac{k_B T}{i\omega 2\pi a^3\langle \Delta\theta^2(\omega)\rangle}, \tag{2}$$

where $\langle \Delta\theta^2(\omega)\rangle$ is the mean squared angular displacement in the frequency domain [10].

Then, microrheological methods relay upon the accurate determination of either the translational or the rotational particles's mean squared displacement (MSD). A number of different techniques such as single and multiple light scattering, optical and confocal microscopy, atomic force microscopy, are available to measure those quantities in different experimental conditions. Naturally, some are better suited for some situations than others [11–13]. In many systems of interest, such as solutions of filamentous proteins, DNA, polymers, etc., the matrix could itself scatter light significantly and/or it can contain highly light-scattering components as it is the case of living cells. Thus one needs to develop efficient experimental methods capable to distinguish the motion of the probes from that of the materials components. In a previous work [9], we have shown that the microrheology of viscoelastic media, such as polymer solutions, obtained from the rotational motion of spherical probes coincides with that obtained from the translational motion of the same probes and with mechanical measurements, when the mesh size of the polymer network is much smaller than the probes size. There, we use optically anisotropic spherical particles as the probes and depolarized dynamic light scattering (DDLS) to determine both the translational and the rotational MSD simultaneously. As we pointed out in Ref. [9], the intrinsic light-scattering power of the system studied there (aqueous solution of polyacrylamide of high molecular weight), could be sufficiently high to mask measurements performed by usual dynamic light scattering. However, as we noted in that work, DDLS from optically anisotropic probes allows us to suppress the background signal when the system of interest scatters light but does not depolarize it. In the present work we investigate in more detail the limits of such a method. Here we present experimental results for the microrheology of viscoelastic fluids whose light-scattering capability is varied by adding inclusions. As in our previous work, we use DDLS to measure the rotational and translational motion of optically anisotropic probe particles embedded in those flu-

ids. As in [9], the systems studied here are polyacrylamide polymers of high molecular weight dissolved in water. The inclusions are polystyrene spheres, of diameter 1 μm, dispersed in the solution at various volume fractions. In the following section we describe details of the sample preparation, experimental techniques, and data analysis. In Sec. III, we present and discuss our results.

II. METHODS

A. Sample preparation

Polymeric solutions are prepared by dissolving polyacrylamide (Sigma), molecular weight $M_W=5-6\times10^6$ g/mol, in deionized water of resistivity 17.0 MΩ cm. Polystyrene spherical particles (PS) of diameter 1 μm dispersed in the solution at various volume fractions ϕ_{PS}, serve as highly light-scattering inclusions. The probe particles are optically anisotropic spherical particles made of liquid crystals (LC) of diameter 430 nm. The probes are dispersed in the solution at a very low volume fraction $\phi_{LC}\approx10^{-5}$ to avoid interaction between them and with the inclusions. The probes are made by emulsification of liquid crystal (RM257, Merck) in water at the temperature of the nematic phase as follows: 0.2 g of reactive monomer RM257 and 0.1 g of photoinitiator Darocur 1173 (Ciba) are dissolved in 20 g of ethanol at room temperature. The mixture is then injected into stirring water, producing a polydisperse dispersion of liquid crystalline (with photoinitiator) droplets in water. The system is allowed to equilibrate at 80 °C, above the temperature of the crystal-nematic phase transition of the monomer. The photoinitiator is activated by irradiation with UV light, which polymerizes the monomer, freezing the internal nematic order in the droplet [14,15]. We corroborated that the probes were solid spheres with optical anisotropy, after UV irradiation, by drying a drop of the suspension and observing the particles by optical microscopy. Images of the particles as seen between crossed polarizers can be found in [15]. Suspensions of the anisotropic particles with low polydispersity are obtained by fractionation, following the depletion crystallization method of Bibette [16]. In the present work, we use probe particles of hydrodynamic diameter 430 nm, which is the more abundant species in the batch, with a size polydispersity of 10%. Mechanical measurements of the viscoelastic moduli are carried out using the concentric cylinders geometry in a Paar-Physica MCR300 rheometer. All experiments are performed at a constant temperature of 23 °C. The mesh size ξ of the polymeric network is estimated as $\xi=R_G(c^*/c)^{3/4}$ [17], where R_G is the radius of gyration, c and c^* are the polymer concentration and its critical value, respectively. The latter is determined as the concentration at the onset of the power law behavior of the low shear viscosity vs c. We find ξ to be in the range of 1–9 nm for matrices with polymer concentration in the range of 0.8–0.1 % weight by weight (w/w) studied here. Thus the mesh size associated with the polymer network is much smaller than the probe particle's size, which is a necessary condition to avoid caging effects of the tracer particles. Figure 1 shows the low-shear viscosity η of the polymeric solution for a range of polymer concentrations. As one can see here, there is a clear change in the slope of the viscosity at the polymer concentration $c^*\approx7\times10^{-3}$% (w/w), referred to as the critical concentration, where the solution changes from dilute to semidilute.

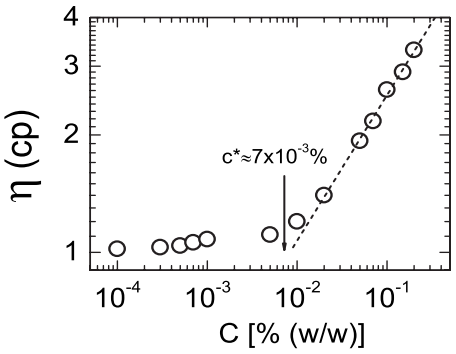

FIG. 1. The critical polymer concentration c^* is determined as the concentration at the onset of the power law behavior of the viscosity η as a function of polymer concentration c.

B. Depolarized dynamic light scattering

Depolarized dynamic light scattering can be used to measure simultaneously the translational and rotational dynamics of anisotropic particles. The setup used in this work is standard. The sample is placed in a goniometer (Brookhaven) in the center of an optical vat filled with index matching fluid (decalin). A polarized laser beam of wavelength $\lambda=488$ nm is focused onto the sample cell. The direction of the x and z axis of the laboratory-fixed frame are defined by the direction of the wave vector of the incident light $\boldsymbol{k}_i$ and by the direction of its polarization $\boldsymbol{n}$, respectively. The light scattered at an angle θ with respect to the axis x is collected by a monomode optical fiber located on the x-y (scattering) plane. A second polarizer is located before the optical fiber to ensure that only one mode reaches the detector. The scattered light is split and directed to two photon detectors (ALV/SO-SIPD), and the signal is processed by a time correlator (ALV 6010/160) operated in the pseudocross-correlation mode. The output of the correlator is $g^{(2)}(k,t)$, the time correlation function of the scattered light intensity $I(k,t)$ with wave vector $k=(4\pi n_s/\lambda)\sin(\theta/2)$, i.e.,

$$g_T^{(2)}(k,t)=\langle I(k,0)I(k,t)\rangle/\langle I(k,0)\rangle^2, \tag{3}$$

where n_s is the refraction index of the medium, t is the lag time, and the angular brackets mean a time average [15,18].

The nematiclike internal structure of the optically anisotropic *LC* particles allows us to assume a cylindrical symmetry of the polarizability tensor $\boldsymbol{\alpha}$. Its diagonal components are $\alpha_\parallel$, $\alpha_\perp$, and $\alpha_\perp$ in the particle-fixed frame with the x component pointing in the direction of the particle director $\hat{\mathbf{u}}(t)$, a unit vector whose direction, as seen from the laboratory-fixed frame, changes randomly due to fluctuating torques exerted by the solvent molecules. The anisotropy of the scattering particles depolarizes the incident light and one can measure separately the parallel $E_{VV}(k,t)$ and perpendicular $E_{VH}(k,t)$ components, with respect to the direction of the incident polarization, of the scattered electrical field by using

the optical setup with the polarization directors of both polarizers vertical (VV) or with the first vertical and the second horizontal (VH), respectively. The electrical field components fluctuate due to the random translational and rotational motion of the particles and one can define two different correlation functions between these components of the scattered electrical field, namely,

$$g_{VV}^{(1)}(k,t) = \langle E_{VV}^{*}(k,0)E_{VV}(k,t)\rangle / \langle |E_{VV}(k,0)|^2 \rangle \tag{4}$$

and

$$g_{VH}^{(1)}(k,t) = \langle E_{VH}^{*}(k,0)E_{VH}(k,t)\rangle / \langle |E_{VH}(k,0)|^2 \rangle . \tag{5}$$

With the assumption of independence between the translational and the rotational dynamics, we have for spherical particles [18]

$$g_{VV}^{(1)}(k,t) = [A + Bf_R(t)]f(k,t) \tag{6}$$

and

$$g_{VH}^{(1)}(k,t) = f_R(t)f(k,t), \tag{7}$$

where $f_R(t)$ and $f(k,t)$ are the dynamic correlation functions describing rotational and translational motion of single particles in the host matrix, respectively. The field correlation functions, Eqs. (6) and (7), for each polarizer's geometry are obtained from the corresponding intensity correlation functions via the Siegert relation, i.e., $g^{(2)}(k,t)=1+b|g^{(1)}(k,t)|^2$, where b is an experimental constant of order 1 [18]. The constants A and B in Eq. (6) depend only on the components of the polarizability tensor which are intrinsic particle properties and can be measured in a known host fluid [15], $A=45\alpha^2/(45\alpha^2+4\beta^2)$ and $B=4\beta^2/(45\alpha^2+4\beta^2)$, where $\alpha=\frac{1}{3}(\alpha_{\parallel}+2\alpha_{\perp})$ and $\beta=\alpha_{\parallel}-\alpha_{\perp}$ represent the isotropic and the anisotropic parts of the polarizability tensor. In this work, those constants are determined by light scattering from particles in water, using the condition $A+B=1$ and the ratio $(\alpha/\beta)^2=(3\langle I_{VV}\rangle-4\langle I_{VH}\rangle)/45\langle I_{VH}\rangle$ [18].

Although the rotational and translational dynamics are mixed up in the field correlation functions, one can see from Eqs. (6) and (7) that the dynamic correlation functions can be obtained either by measuring both $g_{VV}^{(1)}(k,t)$ and $g_{VH}^{(1)}(k,t)$ at the same scattering angle, or by measuring $g_{VH}^{(1)}(k,t)$ at two different scattering angles. As we show below, both possibilities can be realized and both lead to the same results in the absence of inclusions and at low polymer concentrations, when the light scattered by the polymer matrix is only a few percent of the light scattered by the probe particles. On the contrary, in the presence of inclusions and/or more concentrated polymeric matrices having a higher scattering power, the second option provides a method to block the light scattered by the medium, avoiding spurious signal from reaching the detector. The mean squared displacements, rotational and translational, can be obtained from the dynamic correlation functions by using the Gaussian approximation, i.e., we assume $f(k,t)=\exp[-k^2W(t)]$ and $f_R(t)=\exp[-6\Omega(t)]$ [19], where $W(t)=\langle \Delta \mathbf{r}^2(t)\rangle/6$ and $\Omega(t)=\langle \Delta\theta^2(t)\rangle/4$.

C. Data analysis

Mechanical properties of the systems studied here are determined from the measured mean squared displacements, rotational and translational, following the method devised by Dasgupta *et al.* [20]. Here, we reproduce only the equations used in the analysis of our data. Thus the storage and the loss moduli are obtained as follows:

$$G'(\omega) = G(\omega)\{1/[1+\beta'(\omega)]\} \times \cos\left[\frac{\pi\alpha'(\omega)}{2} - \beta'(\omega)\alpha'(\omega)\left(\frac{\pi}{2}-1\right)\right], \tag{8}$$

$$G''(\omega) = G(\omega)\{1/[1+\beta'(\omega)]\} \times \sin\left[\frac{\pi\alpha'(\omega)}{2} - \beta'(\omega)[1-\alpha'(\omega)]\left(\frac{\pi}{2}-1\right)\right], \tag{9}$$

where

$$G(\omega) = \frac{k_B T}{\pi a \langle \Delta r^2(\omega)\rangle \Gamma[1+\alpha(\omega)][1+\beta(\omega)/2]}. \tag{10}$$

Here, $\langle \Delta r^2(\omega)\rangle$ denotes the magnitude of $\langle \Delta \mathbf{r}^2(t)\rangle$ evaluated at $t=1/\omega$ and $\alpha(\omega)$ and $\beta(\omega)$ are the first and second order logarithmic time derivative of the MSD, respectively, i.e., $\alpha(\omega)=[\partial \ln\langle \Delta r^2(t)\rangle/\partial \ln t]_{t=1/\omega}$ and $\beta(\omega)=[\partial^2 \ln\langle \Delta r^2(t)\rangle/\partial \ln t^2]_{t=1/\omega}$. Similarly, $\alpha'(\omega)$ and $\beta'(\omega)$ are the first and second order logarithmic derivatives of $G(\omega)$, respectively.

III. RESULTS

The samples we study are aqueous dispersions of polyacrylamide at a concentration of 0.5% (w/w), where LC particles are used as tracer particles. Additionally, different amounts of latex particles (the inclusions) are added to the samples in order to vary the ratio between light scattered by the probe particles and by the host medium. The inclusions' volume fraction is varied from 10^{-6} to 5×10^{-5}. For $\phi_{PS} \geqslant 0$, up to $\approx 10^{-5}$, the average intensity measured in the VH configuration is the same as without inclusions. However, for volume fractions $\approx 5\times10^{-5}$ or above, there is an additional contribution due to multiple scattering from the inclusions.

Although the main interest here is to study the effect of the inclusions, for comparison let us consider first the case without them, i.e., $\phi_{PS}=0$. In this case most of the light scattered by the sample comes from the probe particles, and traditional single light-scattering microrheology in both geometries, VV and VH, leads to equivalent results [9]. Figure 2 shows the time correlation functions measured using both geometries, obtained as the time average of data collected for 1–3 h, depending on the decay time and count rate. As a reference, we have also plotted the intensity correlation function of LC particles dispersed in water. As we can see, the decay time of the correlation function corresponding to the tracers immersed in the polymer solution is, approximately, a decade longer than that corresponding to those dispersed in water, meaning that the presence of the polymer slows down the motion of the particles. Figure 3 shows the translational

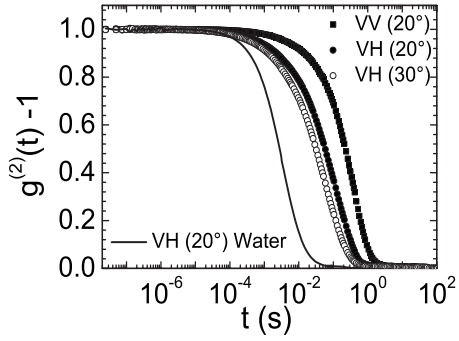

FIG. 2. Time correlation function of the light scattered from optically anisotropic spherical particles dispersed in water (line) and in aqueous solutions of polyacrylamide at a concentration of 0.5% (w/w) (symbols).

and rotational mean squared displacements corresponding to the system in Fig. 2, measured using both procedures mentioned in the previous section. Open symbols represent the mean squared displacements extracted from measurements in the VH configuration at two different scattering angles, 20° and 30°, whereas solid symbols correspond to the measurements in VV and in VH configurations at the same scattering angle, 20°. As one can see here, both procedures lead to similar results. Furthermore, one can also notice here that the data for the rotational motion resemble those corresponding to the translational case. In fact, if we normalize $\langle \Delta \boldsymbol{r}^2(t) \rangle$ by $2a^2$, the resulting curve is very similar to the one for $\langle \Delta \theta^2(t) \rangle$. This indicates already that the microrheology obtained from rotational diffusion will coincide with that from translational diffusion, as can be deduced from Eqs. (1) and (2). In Fig. 4 we compare the storage (open squares) and loss (open circles) moduli measured using a mechanical rheometer with those determined by microrheology experiments (lines). In Fig. 4(a), lines correspond to the moduli obtained from the translational mean squared displacement and in Fig. 4(b) to those from the rotational mean squared displacement. This level of agreement between optical microrheology, from both translation and rotation, with mechanical measurements has been previously reported [9].

Let us now present and discuss our results when the host matrix has itself a high light-scattering power, which in our

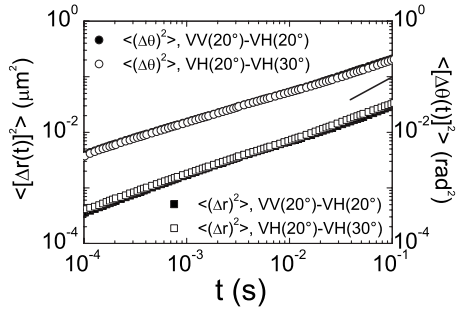

FIG. 3. Translational and rotational mean squared displacements of LC particles, measured using the optical configurations as indicated in Fig. 2. The line represents a slope of 1. As it can be seen, both mean squared displacements have slope lower than 1, indicative of viscoelastic relaxation processes in the medium.

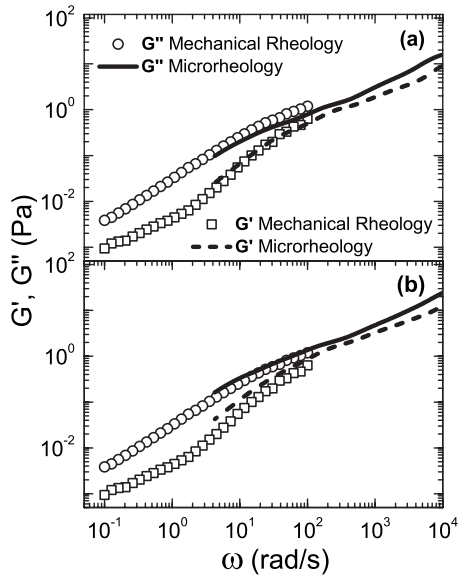

FIG. 4. Comparison of the storage G' and loss G'' moduli of the sample in Fig. 3, measured by translational (a) and rotational (b) probe diffusion microrheology (lines) and mechanical rheology (symbols).

case is provided by the presence of 1-μm polystyrene spheres in the medium. We examine samples where $\phi_{PS} \approx 10^{-6}$, 5×10^{-6}, 10^{-5}, and 5×10^{-5}. For this set of samples, the ratio between the light scattered by the system containing only the inclusions and containing both inclusions and probes is 0.29, 0.47, 0.64, and 0.80, respectively, when measured in the VV configuration at 30°. Thus, in such cases, the inclusions' contribution to the VV component of the scattered light becomes important and masks the dynamics of the probes. As we show below, such inconvenience is overcome when the dynamic correlation functions $f(k,t)$ and $f_R(t)$ are determined from $g_{VH}(k,t)$, measured by depolarized dynamic light scattering at two different angles. This method assumes that the depolarization of light is due only to the rotational

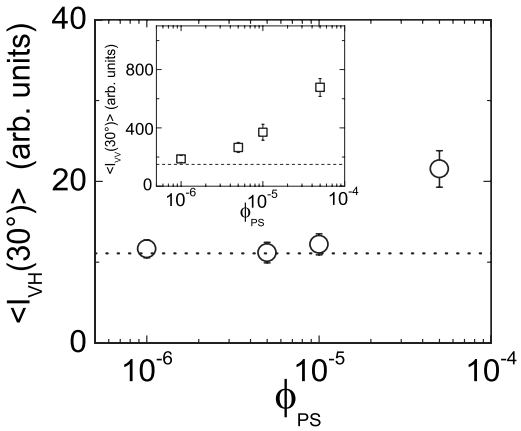

FIG. 5. Intensity of the light scattered at 30°, measured in the VH configuration, as a function of the polystyrene spheres volume fraction (open symbols). The inset shows the results corresponding to measurements performed in the VV configuration. Lines represent the case ϕ_{PS}=0.

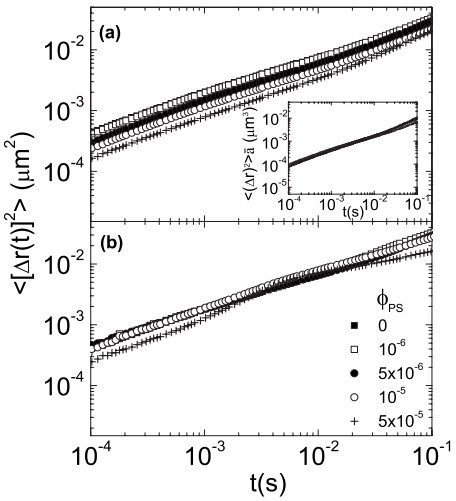

FIG. 6. Translational mean squared displacement of optically anisotropic probe particles embedded in matrices containing different volume fractions ϕ_{PS} of latex particles (symbols) measured: (a) in the VV-VH geometry at 30° and (b) in the VH-VH geometry at two different angles, 20° and 30°. The inset shows the scaled mean squared displacements.

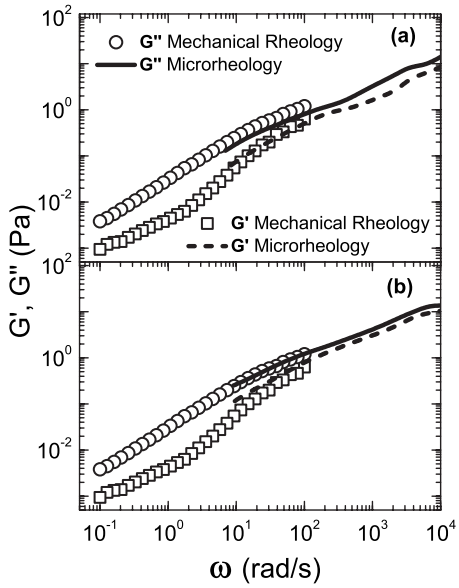

FIG. 7. Comparison of storage G' and loss G'' moduli of the sample with $\phi_{PS} \approx 10^{-5}$, as measured in the VH-VH scheme by (a) translational and (b) rotational probe diffusion microrheology (lines), and by mechanical rheology (symbols).

motion of the probes. As we show in Fig. 5, such a condition is fulfilled by the systems studied here. Figure 5 shows the intensity of the light scattered (at 30°) by samples containing the probes and the inclusions at different volume fractions. The symbols represent the total light scattered from the system, i.e., the contributions from the polymer solution containing the probes and the inclusions. The lines represent the light scattered by the solution containing only the probes. As one can see here, in the VH configuration the contribution from the inclusions is vanishing small in the range $\phi_{PS} = 0 - 10^{-5}$. Let us note here that in this configuration the light scattered from the polymer solution is practically zero. Thus the dashed line is basically the intensity of the light scattered by the probes. The inset shows the corresponding results for the measurements performed in the VV configuration. As it was mentioned above, in this case there is a strong contribution from the inclusions which increases as ϕ_{PS} increases. In this configuration, the polymer solution also contributes with about 10% of the light scattered from the solution including only the probes (solid line). We should note that this scheme, however, will fail to provide reliable results if a significant amount of light is depolarized by the sample itself or by other means, for instance in the case of multiple light scattering, unless care is taken to account for those effects.

Figure 6 shows a comparison of the translational mean squared displacement of the anisotropic particles, in the samples with and without inclusions, determined by measuring both $g_{VV}(k,t)$ and $g_{VH}(k,t)$ at the same scattering angle (scheme VV-VH) and by measuring $g_{VH}(k,t)$ at two angles (scheme VH-VH). Figure 6(a) shows the results obtained in the scheme VV-VH at 30°. As one can see here, in the sample where $\phi_{PS} = 10^{-6}$ the MSD is almost identical to that in the sample without inclusions, the curves fall practically on top of each other. However, as the concentration of inclusions is increased further, the MSD is shifted downward more for higher values of ϕ_{PS}. Since in these cases there is an increasing contribution of the inclusions to the scattering of light in the parallel polarization configuration, the decay of the light intensity correlation function is caused by the motion of both species, the probes and the inclusions. Therefore the (apparent) MSD determined in this way is not the actual mean squared displacement of the probes, but a rather complex combination of the MSD of both types of particles. Let us note, however, that the change in the MSD appears to be only in its magnitude, not in its shape. In fact, we found that the mean squared displacement can be scaled by an effective radius $\bar{a}$, determined as the average size of both types of particles (the probes and the inclusions), weighted by its corresponding concentration. The effective radius ranges from 0.215 μm (the radius of the liquid crystal particles), for the sample without inclusions, to a value around 0.5 μm (the radius of the polystyrene particles). As one can see in the inset, the scaled MSD's $[\langle \Delta \boldsymbol{r}^2(t) \rangle \bar{a}]$ collapse to a single curve, except for the system with $\phi_{PS} \approx 5 \times 10^{-5}$ where multiple scattering of light is observed.

Figure 6(b) shows the results from the VH-VH scheme at 20° and 30°. As one can see here, in this scheme the resulting MSD's coincide within the experimental error (which is within the symbol size), except again for the system with the highest concentration of inclusions where there is an additional contribution to the depolarization of light from multiple light scattering. In fact, the mean squared displacement obtained for this sample shows a different time dependence leading to completely different microrheology results. The rotational MSD's exhibit a similar behavior, i.e., they are shifted (upwards in this case) as the concentration of inclusions increases when measured using the VV-VH scheme, but they coincide in the VH-VH scheme, except for the system with $\phi_{PS} \approx 5 \times 10^{-5}$.

In Fig. 7 we present the microrheology results for G' and G'', obtained from the analysis of both the translational (a)

and the rotational (b) diffusion of the probe particles, measured in the VH-VH scheme. These results correspond to measurements performed in the sample with the highest concentration of inclusions where multiple scattering is still negligible, namely, the system with $\phi_{PS} \approx 10^{-5}$. However, as one can see from Fig. 6(b), the results obtained from systems with lower concentrations of inclusions would be practically the same as those presented here. Furthermore, given the correspondence, by a factor of $2a^2$, between the translational and the rotational MSD's, the results from both diffusion motions are essentially the same. For comparison, in Fig. 7 we present also the mechanical measurements. We verified that the presence of the inclusions does not affect the rheology of the polyacrylamide solutions. We found similar mechanical results for the elastic and viscous moduli measured in samples without inclusions and with added polystyrene spheres at a volume fraction of 10^{-4}, which is higher than the highest concentration used for the optical experiments. Figure 7(a) shows that comparison when the microrheology is performed using the translational MSD, whereas Fig. 7(b) shows the corresponding comparison for the rotational MSD. As one can see here, the agreement with mechanical results is excellent in the range of frequencies where both techniques overlap. These results demonstrate the feasibility to use light scattering techniques to measure the rheology of viscoelastic media with high scattering power. Under the conditions of our experiment, we found that one can obtain reliable results even when the intensity of the light scattered by the matrix (in our case due to the inclusions) is as high as 65% of the total. Other experimental conditions will set a different value. The method assumes single scattering of light. Thus it is limited to conditions where multiple light scattering, either from the matrix or from the probes, is negligible. In principle, more turbid complex media could be studied by DDLS if single scattering events could be isolated from the measured depolarized intensity by using cross-correlation detection schemes [21,22].

IV. CONCLUSIONS

In this work we show that depolarized dynamic light scattering from optically anisotropic spherical tracer particles is a suitable technique to determine the rheology of strongly light-scattering media. This is possible when the total depolarized scattered light, as long as it is free from multiple scattering, is only due to the dynamics of the tracer particles as is the case of the system studied here. Our results suggest that DDLS could be useful to study systems where intrinsical inclusions are present, perhaps even in complex systems such as living biological cells.

ACKNOWLEDGMENTS

This work was supported by the Consejo Nacional de Ciencia y Tecnología, México, Grant Nos. 46121-F and U47611-F.

[1] R. E. Mahaffy, C. K. Shih, F. C. MacKintosh, and J. Käs, Phys. Rev. Lett. **85**, 880 (2000).
[2] S. Yamada, D. Wirtz, and S. C. Kuo, Biophys. J. **78**, 1736 (2000).
[3] C. Wilhelm, F. Gazeau, and J. C. Bacri, Phys. Rev. E **67**, 061908 (2003).
[4] A. W. C. Lau, B. D. Hoffmann, A. Davies, J. C. Crocker, and T. C. Lubensky, Phys. Rev. Lett. **91**, 198101 (2003).
[5] T. G. Mason and D. A. Weitz, Phys. Rev. Lett. **74**, 1250 (1995).
[6] T. G. Mason, K. Ganesan, J. H. van Zanten, D. Wirtz, and S. C. Kuo, Phys. Rev. Lett. **79**, 3282 (1997).
[7] F. Scheffold, S. Romer, F. Cardinaux, H. Bissig, A. Stradner, L. F. Rojas-Ochoa, V. Trappe, C. Urban, S. E. Skipetrov, L. Cipelletti, and P. Schurtenberger, Prog. Colloid Polym. Sci. **123**, 141 (2004).
[8] A. Papagiannopoulos, C. M. Fernyhough, and T. A. Waigh, J. Chem. Phys. **123**, 214904 (2005).
[9] E. Andablo-Reyes, P. Díaz-Leyva, and J. L. Arauz-Lara, Phys. Rev. Lett. **94**, 106001 (2005).
[10] Z. Cheng and T. G. Mason, Phys. Rev. Lett. **90**, 018304 (2003).
[11] M. L. Gardel, M. T. Valentine, and D. A. Weitz, *"Microrheology" in Microscale Diagnostic Techniques* (Kenny Breuer, Springer-Verlag, New York, 2005).
[12] A. D. Dinsmore, E. R. Weeks, V. Prasad, A. C. Levitt, and D. A. Weitz, Appl. Opt. **40**, 4152 (2001).
[13] M. L. Gardel, M. T. Valentine, J. C. Crocker, A. R. Bausch, and D. A. Weitz, Phys. Rev. Lett. **91**, 158302 (2003).
[14] A. Mertelj, J. L. Arauz-Lara, G. Maret, T. Gisler, and H. Stark, Europhys. Lett. **59**, 337 (2002).
[15] P. Díaz-Leyva, E. Pérez, and J. L. Arauz-Lara, J. Chem. Phys. **121**, 9103 (2004).
[16] J. Bibette, J. Colloid Interface Sci. **147**, 474 (1991).
[17] E. C. Cooper, P. Johnson, and A. M. Donald, Polymer **32**, 2815 (1991).
[18] B. J. Berne and R. Pecora, *Dynamic Light Scattering: With Applications to Chemistry, Biology and Physics* (John Wiley, New York, 1976).
[19] V. Degiorgio, R. Piazza, and R. B. Jones, Phys. Rev. E **52**, 2707 (1995).
[20] B. R. Dasgupta, S. Y. Tee, J. C. Crocker, B. J. Frisken, and D. A. Weitz, Phys. Rev. E **65**, 051505 (2002).
[21] C. Urban and P. Schurtenberger, J. Colloid Interface Sci. **207**, 150 (1998).
[22] A. Moussaïd and P. N. Pusey, Phys. Rev. E **60**, 5670 (1999).